A 40-y record reveals gradual Antarctic sea ice increases followed by decreases at rates far exceeding the rates seen in the Arctic

Claire L. Parkinson[a,1]

[a]Cryospheric Sciences Laboratory/Code 615, NASA Goddard Space Flight Center, Greenbelt, MD 20771

This contribution is part of the special series of Inaugural Articles by members of the National Academy of Sciences elected in 2016.

Contributed by Claire L. Parkinson, May 24, 2019 (sent for review April 16, 2019; reviewed by Will Hobbs and Douglas G. Martinson)

Following over 3 decades of gradual but uneven increases in sea ice coverage, the yearly average Antarctic sea ice extents reached a record high of 12.8 × 10^6 km^2 in 2014, followed by a decline so precipitous that they reached their lowest value in the 40-y 1979–2018 satellite multichannel passive-microwave record, 10.7 × 10^6 km^2, in 2017. In contrast, it took the Arctic sea ice cover a full 3 decades to register a loss that great in yearly average ice extents. Still, when considering the 40-y record as a whole, the Antarctic sea ice continues to have a positive overall trend in yearly average ice extents, although at 11,300 ± 5,300 km^2·y^{-1}, this trend is only 50% of the trend for 1979–2014, before the precipitous decline. Four of the 5 sectors into which the Antarctic sea ice cover is divided all also have 40-y positive trends that are well reduced from their 2014–2017 values. The one anomalous sector in this regard, the Bellingshausen/Amundsen Seas, has a 40-y negative trend, with the yearly average ice extents decreasing overall in the first 3 decades, reaching a minimum in 2007, and exhibiting an overall upward trend since 2007 (i.e., reflecting a reversal in the opposite direction from the other 4 sectors and the Antarctic sea ice cover as a whole).

sea ice | climate change | satellite Earth observations | climate trends | Antarctic sea ice

Since the late 1990s, it has been clear that the Arctic sea ice cover has been decreasing in extent over the course of the multichannel passive-microwave satellite record begun in late 1978 (1–3). The decreases have accelerated since the 1990s and have been part of a consistent suite of changes in the Arctic, including rising atmospheric temperatures, melting land ice, thawing permafrost, longer growing seasons, increased coastal erosion, and warming oceans (4, 5). Overall, it has been a consistent picture solidly in line with the expectations of the warming climate predicted from increases in greenhouse gases. In particular, modeled sea ice predictions showed marked Arctic sea ice decreases, and the actual decreases even exceeded what the models predicted (6).

The Antarctic situation has been quite different, with sea ice extent increasing overall for much of the period since 1978 (7–11). These increases have been far more puzzling than the Arctic sea ice decreases and have led to a variety of suggested explanations, from ties to the ozone hole (12, 13; rejected in refs. 14, 15); to ties to the El Niño–Southern Oscillation (ENSO) (16), the Interdecadal Pacific Oscillation (17), and/or the Amundsen Sea Low (10, 13, 17); to ties to basal meltwater from the ice shelves (18; rejected in ref. 19). None of these has yet yielded a consensus view of why the long-term Antarctic sea ice increases occurred.

In the meantime, while the unexpected, decades-long overall increases in Antarctic sea ice extent are still being puzzled out, the sea ice extent has taken a dramatic turn from relatively gradual increases to rapid decreases. On a yearly average basis, the peak sea ice extent since 1978 came in 2014. Since then, the decreases have been so great that the yearly averages for 2017 and 2018 are the lowest in the entire 1979–2018 record, essentially wiping out the 35 y of overall ice extent increases in just a few years. This dramatic reversal in the changes occurring in the Antarctic sea ice will provide valuable further information to test earlier suggested explanations of the long-term Antarctic sea ice increases. We now have a 40-y multichannel passive-microwave satellite record of the Antarctic sea ice cover, all of which resides in the Southern Ocean. The purpose of this paper is to present that record both for the Southern Ocean as a whole (labeled "Southern Hemisphere" in the figures, to emphasize the inclusion of the entire hemispheric sea ice cover) and for the breakdown of the Southern Ocean into the 5 sectors identified in Fig. 1.

Data and Methods

The data used throughout this paper come from a satellite-based multichannel passive-microwave data record begun in late 1978 following the October 24, 1978 launch of the scanning multichannel microwave radiometer (SMMR) on NASA's Nimbus 7 satellite. The SMMR data are used in this study for 1979 through mid-August 1987, followed by data from a sequence of the US Department of Defense's Defense Meteorological Satellite Program (DMSP) special sensor microwave imager (SSMI) instruments, the first of which was launched on the DMSP F8 satellite on June 18, 1987, and the follow-on DMSP SSMI sounder (SSMIS) instruments, the first of which was launched on the DMSP F16 satellite on October 18, 2003. Details on the intercalibration between the data from successive instruments, to obtain a consistent long-term record, can be found in reports by Cavalieri et al. (20, 21).

Satellite passive-microwave data have major advantages over other data for studies of changes in the extent and distribution of the Antarctic sea ice cover in recent decades. First, satellites allow monitoring of the full Antarctic sea ice cover every 1 or 2 d. Second, the satellite passive-microwave record

Significance

A newly completed 40-y record of satellite observations is used to quantify changes in Antarctic sea ice coverage since the late 1970s. Sea ice spreads over vast areas and has major impacts on the rest of the climate system, reflecting solar radiation and restricting ocean/atmosphere exchanges. The satellite record reveals that a gradual, decades-long overall increase in Antarctic sea ice extents reversed in 2014, with subsequent rates of decrease in 2014–2017 far exceeding the more widely publicized decay rates experienced in the Arctic. The rapid decreases reduced the Antarctic sea ice extents to their lowest values in the 40-y record, both on a yearly average basis (record low in 2017) and on a monthly basis (record low in February 2017).

Author contributions: C.L.P. designed research, performed research, analyzed data, and wrote the paper.

Reviewers: W.H., University of Tasmania; and D.G.M., Columbia University.

The author declares no conflict of interest.

[1]Email: claire.l.parkinson@nasa.gov.

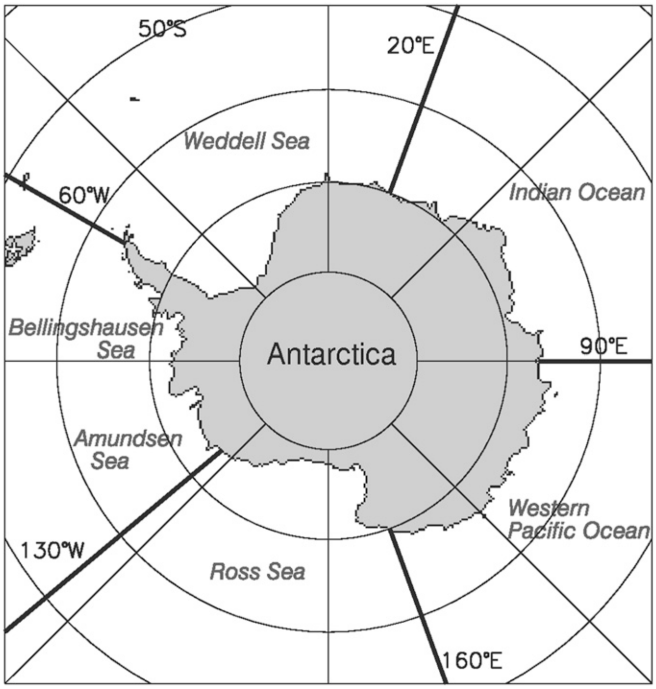

Fig. 1. Identification of the 5 sectors used in the regional analyses. These are identical to the sectors used in previous studies (7, 8).

extends back to the 1970s. Third, the microwave signal from sea ice is quite distinct from the microwave signal from liquid water. Fourth, the microwave radiation is emitted from within the Earth/atmosphere system, rather than being reflected sunlight; hence, the measurements can be made irrespective of day or night conditions. Fifth, at appropriate microwave wavelengths, the microwave radiation from the surface can travel through most cloud covers, allowing measurements under cloudy as well as cloud-free conditions. These advantages result in a 40-y record covering all seasons of the year and allowing determination of large-scale changes in the Southern Ocean sea ice cover that would not be feasible without the satellite passive-microwave data.

The microwave data were converted to sea ice concentrations (percent areal coverages of sea ice) in each pixel (~25 km × 25 km) of the gridded satellite data through the NASA team algorithm described in detail by Gloersen et al. (22). Sea ice extents were then calculated by summing, throughout the region of interest, the areas of each pixel with a calculated sea ice concentration of at least 15%. Ice extents are calculated for each day of available data; yearly and monthly averages are calculated by averaging the daily ice extents for the year or month, respectively. Summer averages are calculated by averaging the daily extents for January, February, and March; autumn averages are calculated by averaging the daily extents for April, May, and June; winter averages are calculated by averaging the daily extents for July, August, and September; and spring averages are calculated by averaging the daily extents for October, November, and December.

Because the sea ice cover has a prominent annual cycle, long-term trends in sea ice extents are more clearly depicted after removing the annual cycle. This is done here both through yearly averaging, which removes considerable additional information as well as the annual cycle (e.g., monthly interannual variability, amplitude of the annual cycle, seasonality of the trends), and through the more information-retaining monthly deviations, calculated by subtracting from the individual month's ice extent the average of the ice extents for that particular month throughout the 40-y record. For example, the monthly deviation for January 1979 is the ice extent for January 1979 minus the average of the ice extents for the 40 months of January 1979–2018.

Trend lines are calculated for the monthly, seasonal, yearly, and monthly deviation datasets through standard linear least squares, and the standard deviations (SDs) of the trends are calculated based on the technique described by Taylor (23). The ratio (R) of the trend magnitude to its SD is given to provide a rough indication of the relative statistical significance of the trends, with higher R values suggesting greater significance. More specifically, if assuming a 2-tailed *t* test and 38 degrees of freedom for the 40-y sea ice record, R values above 2.024 would signify statistical significance at a 95% level or above and R values above 2.712 would signify statistical significance at a 99% level or above; the corresponding values for a 36-y record, also discussed below, are 2.032 and 2.728 for 95% and 99% significance, respectively. In view of the imperfect nature of tests of statistical significance when applied to the real world (24, 25), these numbers are only provided as rough indicators.

The satellite passive-microwave datasets are available at the National Snow and Ice Data Center (NSIDC) in Boulder, CO, and on the NSIDC website, https://nsidc.org (26).

Results

Figs. 2–7 present plots of the monthly averages, monthly deviations, and yearly averages for the Southern Ocean as a whole (Fig. 2) and for each of the 5 sectors it is divided into in Fig. 1 (Figs. 3–7). Table 1 provides details on the yearly average trends and includes values for the 1979–2014 record before the sharp decline in ice extents as well as values for the full 40-y record.

Full Southern Ocean. For the Southern Ocean as a whole, the quite prominent annual cycle has minimum monthly ice extent always (for the 40 y of the dataset, 1979–2018) occurring in February and always well under 5×10^6 km^2 and maximum ice extent occurring in September in all years except 1988, when it was in October, and always well over 17×10^6 km^2 (Fig. 2*A*). The monthly deviations and yearly averages depict clearly the overall upward trend in ice extents until 2014, when the yearly averages reached a record high of 12.8×10^6 km^2, and marked decreases in the subsequent 3 y (Fig. 2 *B* and *C*), leading to a record low monthly average sea ice extent of 2.29×10^6 km^2 in February 2017 (Fig. 2*A*) and a record low yearly average sea ice extent of 10.75×10^6 km^2 in 2017 (Fig. 2*C*). Despite the marked decreases in ice extent following the 2014 record high, the least squares trends remain positive, although at roughly half the magnitude of the 1979–2014 trends (Table 1). Specifically, the 1979–2018 trend of 11,200 ± 2,100 km^2·y^{-1} for the monthly deviations is only 50.7% of the 22,100 ± 2,000 km^2·y^{-1} slope of the trend line for 1979–2014, and the 1979–2018 trend of 11,300 km^2·y^{-1} for the yearly averages is only 50.4% of the trend for 1979–2014 (Table 1).

The 5 sectors also all exhibit a strong annual cycle with monthly ice extent minima frequently in February and maxima frequently in September, although with much greater interannual variability than for the Southern Ocean as a whole. The following sections for the individual sectors highlight some of the regional and interannual variability in the Southern Ocean sea ice cover.

Weddell Sea. In the Weddell Sea, monthly minimum ice extent is always in February, as in the Southern Ocean as a whole, but monthly maximum ice extent varies more frequently from its typical September timing, being in August in 1992, 1994, 2004, and 2017 and in October in 1997, 2002, 2015, and 2018 (Fig. 3*A*). Interestingly, the highest Weddell Sea monthly average ice extent in the 40-y record, in September 1980, was followed the next summer by among the lowest February and March ice extents (Fig. 3*A*), and, similarly, relatively high September values in 1987, 1992, and 2016 were all followed by below average February extents the next year. With other high September ice extents (e.g., in 2007) not being followed by particularly low February extents, this illustrates interannual variability and the difficulty of forecasting ice extents months in advance based simply on current ice extents. High ice extents with low ice concentrations could bring about particularly effective decay seasons, as could winds and ocean currents transporting to the region more warm air and water than normal. Similar to the Southern Ocean as a whole, the Weddell Sea experienced overall ice extent increases, on a yearly average basis, through 2014, although less convincingly (Table 1, with an R value of 1.88 versus the Southern Ocean's R value of 5.25) and with the

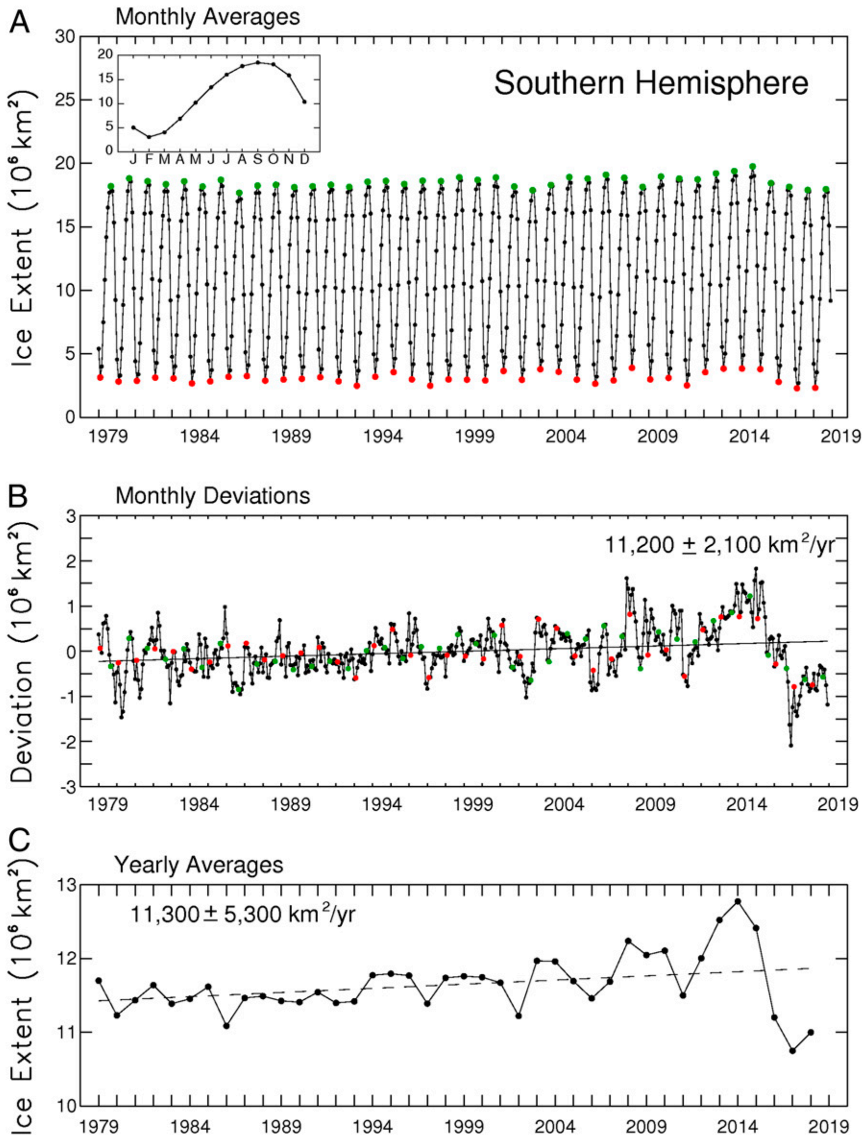

Fig. 2. (*A*) Monthly average sea ice extents for the Southern Hemisphere, January 1979–December 2018. February extents are depicted in red, September extents in green, and all other extents in black. (*Inset*) The 40-y average annual cycle. Single-letter abbreviations are used for months. (*B*) Monthly deviations determined from the monthly average data of *A*, with the same monthly color coding and with the line of linear least squares fit and its slope and SD. (*C*) Yearly average sea ice extents and their line of linear least squares fit. The ice extents are derived from passive-microwave data from the NASA Nimbus 7 and Department of Defense DMSP satellites.

increases continuing, slightly, to 2015 (Fig. 3*C*). The Weddell Sea experienced marked ice extent decreases from 2015–2018, falling just short of reaching its record minimum yearly ice extent set in 1999 (Fig. 3*C*).

Indian Ocean. The Indian Ocean is the one sector in which the average annual cycle of monthly ice extents peaks in October rather than September. Still, its average annual cycle shares with the other sectors a February minimum, making for the most asymmetric of these average cycles, with an 8-mo growth period and a 4-mo decay period (Fig. 4*A*, *Inset*). The month of minimum monthly ice extent was February in all except 2 y (1986 and 2003), when it was March, while the month of maximum ice extent was October in 33 y and September in the remaining 7 y (Fig. 4*A*). The Indian Ocean record high monthly ice extent was reached in October 2010 (Fig. 4*A*), and the year of peak yearly average ice extent was 2010 (Fig. 4*C*), 4 y earlier than the peak for the Southern Ocean as a whole. A decrease in yearly average ice extents from 2010 to 2011 was followed by a rebound in the next 3 y and then a 2-y decrease resulting in the Indian Ocean record minimum yearly ice extent in 2016, before rebounding somewhat in 2017 and 2018 (Fig. 4*C*).

Western Pacific Ocean. Like the Southern Ocean as a whole, the Western Pacific Ocean has a February minimum and a September maximum in its average annual cycle of sea ice extents, although in the Western Pacific case, the October ice is nearly as extensive as the September ice and the August ice is not far behind (Fig. 5*A*, *Inset*). The month of ice extent minimum in the Western Pacific was February in each year except 1980, 1985, 1986, and 2017, when it was March, and the more variable month of maximum was August in 8 y, September in 15 y, and October in 17 y (Fig. 5*A*). The largest deviations from normal came in September and October of 1989, when the ice cover was far less extensive than the average September and October ice covers (Fig. 5*B*). Yearly ice extents in the Western Pacific increased

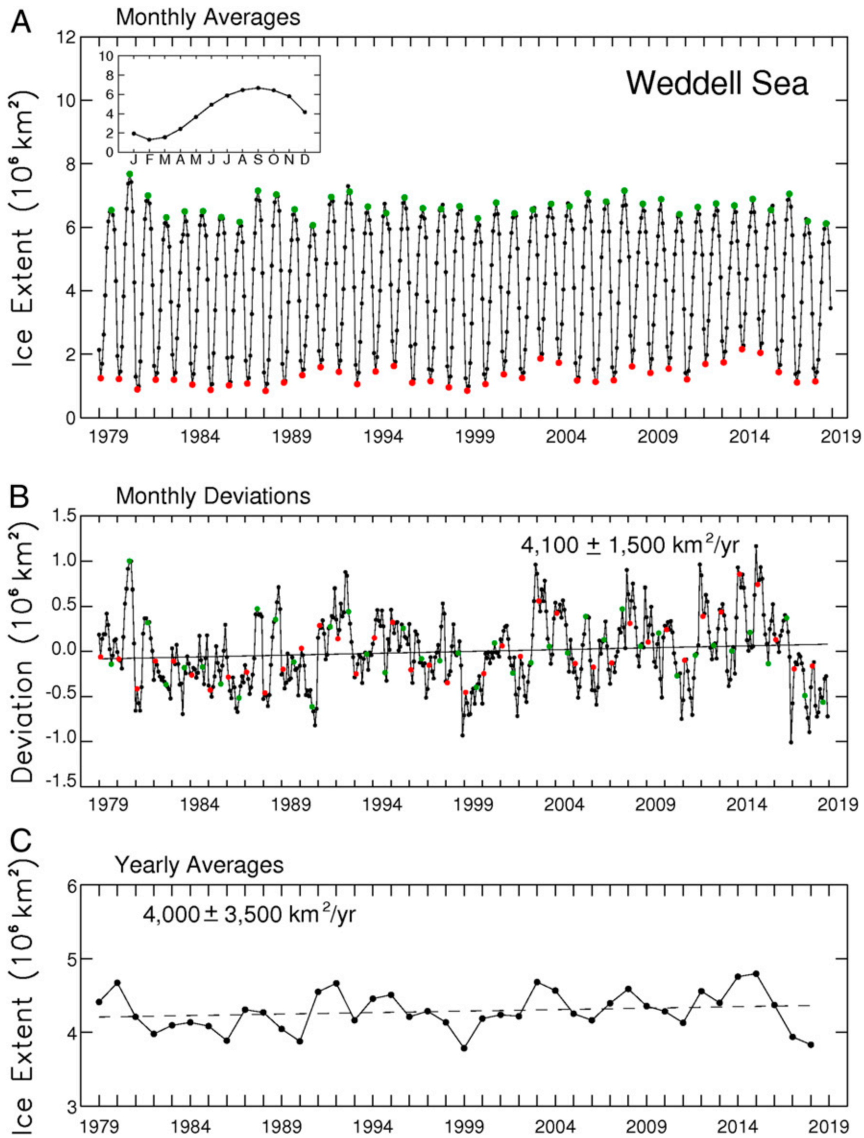

Fig. 3. (*A*) Monthly average sea ice extents in the Weddell Sea, 1979–2018. February extents are colored red, September extents green, and all others black. (*Inset*) The 40-y average annual cycle. (*B*) Monthly deviations, with the line of linear least squares fit and its slope and SD. (*C*) Yearly averages and their line of linear least squares fit.

overall until reaching their record high in 2013, followed by a prominent downward trend from 2013–2018 (Fig. 5*C*). The second highest yearly ice extent came decades earlier, in 1982, which also contained the 2 highest monthly values of the 40-y record, the highest in September 1982 and the second highest in October 1982 (Fig. 5*A*).

Table 1. Slopes and SDs of the lines of linear least squares fit for the yearly sea ice extents in the full Southern Ocean and each of the 5 sectors identified in Fig. 1, both for the 40-y record, 1979–2018, and, in parentheses, for the 36-y record, 1979–2014, before the reversal from overall sea ice increases to rapid decreases

Sector	Slope, 10^3 km^2·y^{-1}	R	Slope, % per decade
Weddell Sea	4.0 ± 3.5 (7.0 ± 3.7)	1.13 (1.88)	1.0 ± 0.8 (1.7 ± 0.9)
Indian Ocean	2.6 ± 1.8 (5.9 ± 1.8)	1.48 (***3.23***)	1.4 ± 0.9 (3.2 ± 1.0)
Western Pacific Ocean	2.6 ± 1.3 (3.2 ± 1.6)	1.96 (1.98)	2.3 ± 1.2 (2.8 ± 1.4)
Ross Sea	5.8 ± 2.9 (11.3 ± 3.0)	1.97 (***3.75***)	2.1 ± 1.1 (4.3 ± 1.1)
Bellingshausen/Amundsen Seas	−3.7 ± 1.8 (−4.9 ± 2.1)	2.02 (*2.32*)	−2.5 ± 1.2 (−3.2 ± 1.4)
Full Southern Ocean	11.3 ± 5.3 (22.4 ± 4.3)	*2.12* (***5.25***)	1.0 ± 0.5 (2.0 ± 0.4)

The slopes and SDs are listed both as the areal loss each year and as the percentage of the ice cover lost each decade. The R column gives the ratio of the slope magnitude for the areal loss to its SD (calculated before rounding to the nearest 100 km^2·y^{-1}), as a rough indicator of statistical significance, both for the 40-y record and, in parentheses, for the 36-y record. Using the 2-tailed *t* test mentioned in the text, statistical significance at the 95% level or above is indicated in the R column by italics and statistical significance at the 99% level or above is indicated by boldface. The trend reversals since 2014 have markedly lessened the statistical significance of the trends.

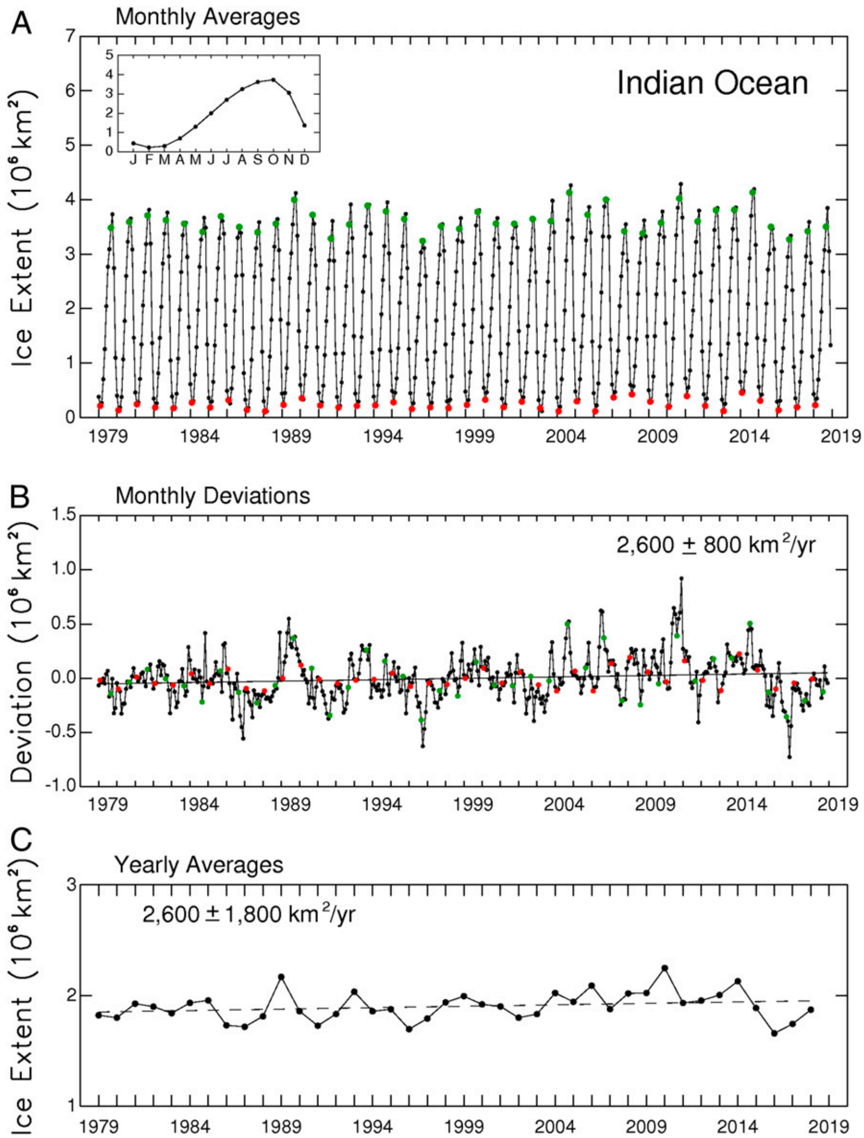

Fig. 4. (*A*) Monthly average sea ice extents in the Indian Ocean, 1979–2018. February extents are colored red, September extents green, and all others black. (*Inset*) The 40-y average annual cycle. (*B*) Monthly deviations, with the line of linear least squares fit and its slope and SD. (*C*) Yearly averages and their line of linear least squares fit.

Ross Sea. The Ross Sea ice extent has a prominent, consistent monthly minimum in February but large variability in its month of maximum, which is July in 3 y, August in 8 y, September in 16 y, October in 12 y, and November in 1 y (Fig. 6*A*). The record high monthly value came in September 2007, although the highest yearly value was much earlier, in 1999 (Fig. 6 *A* and *C*). The overall but nonuniform reduction of sea ice coverage since the 2007 high led to an almost total disappearance of the sea ice cover and record low in February 2017, with some rebounding the following year (Fig. 6*A*). The month that deviated the most from the average annual cycle was December 1979, in a year when the ice cover had been below average since September (Fig. 6*B*). Further interannual variability can be illustrated by the contrast between the September 2007 record high ice extent being followed the next summer by a February also with an unusually high ice extent, versus the high September 1996 ice extent being followed by a low February ice extent (Fig. 6*A*). This phenomenon of high September ice extents being followed sometimes by high and sometimes by low February ice extents is mentioned also in the Weddell Sea section and could be illustrated with many more examples on the sector plots. What happens during the decay season varies greatly depending on the surrounding atmospheric and oceanic conditions.

Bellingshausen/Amundsen Seas. The Bellingshausen/Amundsen Seas is the sector most out of line with the rest of the Southern Ocean, although sharing with each of the sectors the existence of substantial interannual variability (Fig. 7). In 11 y, its month of minimum ice coverage was March rather than February, whereas no other sector had more than 4 y with a minimum month other than February. The large variability in its month of maximum ice extent is more in line with the variability in the other sectors, being July in 2 y, August in 14 y, September in 20 y, and October in 4 y (Fig. 7*A*). However, the major contrast between the Bellingshausen/Amundsen Seas sector and the rest of the Southern Ocean is that it had an overall downward trend in ice extents for most of the record, followed by an overall upward trend. This contrast corresponds well with the marked regional warming recorded on the Antarctic Peninsula, adjacent to the Bellingshausen Sea, for the early decades of the 40-y record (27), a

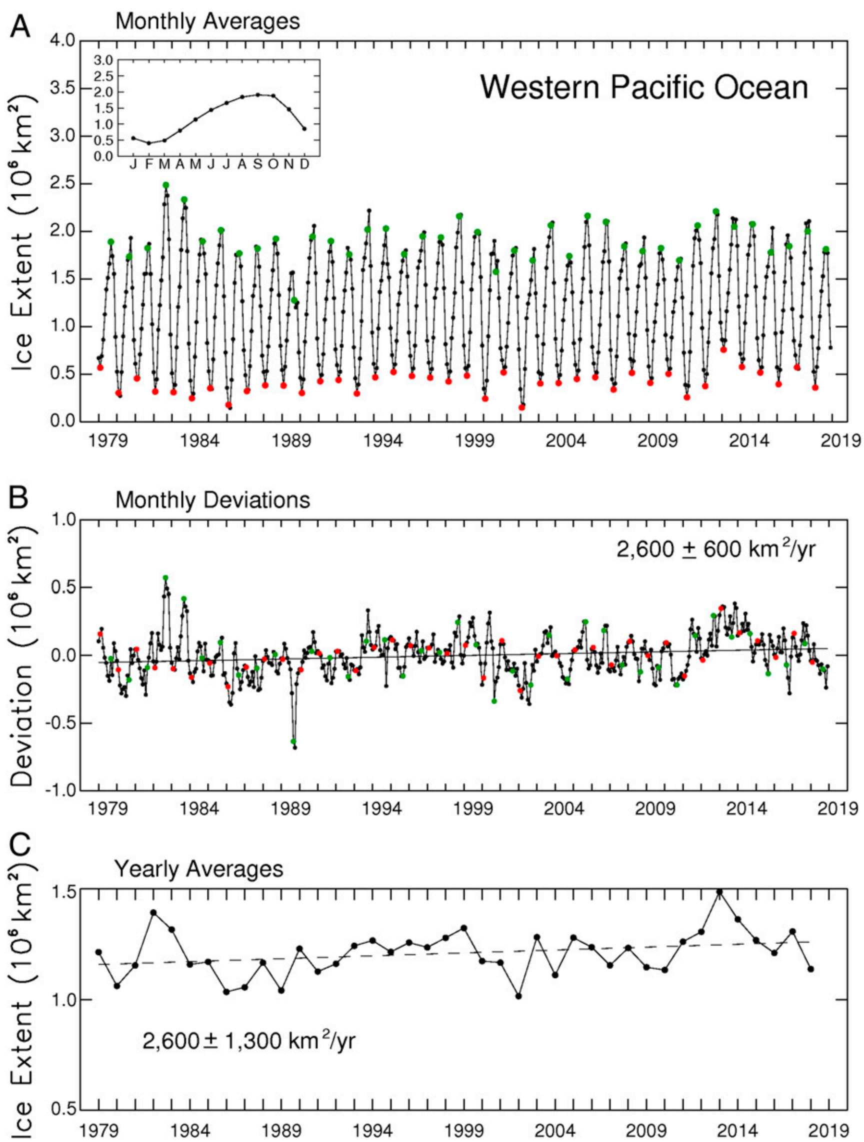

Fig. 5. (*A*) Monthly average sea ice extents in the Western Pacific Ocean, 1979–2018. February extents are colored red, September extents green, and all others black. (*Inset*) The 40-y average annual cycle. (*B*) Monthly deviations, with the line of linear least squares fit and its slope and SD. (*C*) Yearly averages and their line of linear least squares fit.

warming not recorded elsewhere on the continent, and the subsequent cooling over the Antarctic Peninsula (28). The yearly average ice extents in the Bellingshausen/Amundsen Seas reached their minimum in 2007 (Fig. 7*C*), and although the upward trend since 2007 did not result in record high yearly ice extents (Fig. 7*C*), the record high monthly ice extent in the Bellingshausen/Amundsen Seas sector did come late in the record, in September 2015, despite the early decades of overall decreasing sea ice coverage (Fig. 7*A*). The record low ice extent came in March 2010, in line with the general decrease in ice coverage in the first 3 decades of the record and the general increase in ice coverage since then (Fig. 7).

Trends by Month. For the Southern Ocean as a whole, the 40-y sea ice extent trends remain positive for each of the 12 mo (Fig. 8 and Table 2), and hence also for each of the 4 seasons. However, the trend for November is close to 0 and far from statistical significance, at 1,100 ± 6,700 $km^2 \cdot y^{-1}$, and every 40-y monthly trend is far below the trend for the 36-y 1979–2014 period before the recent sea ice declines (Table 2). [All of the monthly trends for the full Southern Ocean were statistically significant at least at the 95% level, and most were also significant at the 99% level, for the 36-y record; for the 40-y record, only 4 remain statistically significant at the 95% level and none are statistically significant at the 99% level (Table 2).] Through 2014, the Indian Ocean, Western Pacific, and Ross Sea all also had positive trends in each month (with ranges of 2,700–8,500 $km^2 \cdot y^{-1}$ in the Indian Ocean, 200–5,700 $km^2 \cdot y^{-1}$ in the Western Pacific, and 3,100–17,700 $km^2 \cdot y^{-1}$ in the Ross Sea), but now, with the full 40-y record, only the Indian Ocean retains that commonality with the full Southern Ocean (Fig. 8). The Western Pacific and Ross Sea now both have 10 mo with positive trends and 2 mo with negative or 0 trends (Fig. 8). The Weddell Sea has negative trends in winter and spring but positive trends in summer and autumn. Once again, the Bellingshausen/Amundsen Seas sector is out of line with the rest of the Southern Ocean, as all 12 of its monthly trends were negative earlier (8), but now with the 40-y record, its summer and autumn values remain negative, whereas its ice extent trends in winter are positive and in autumn are mixed (Fig. 8).

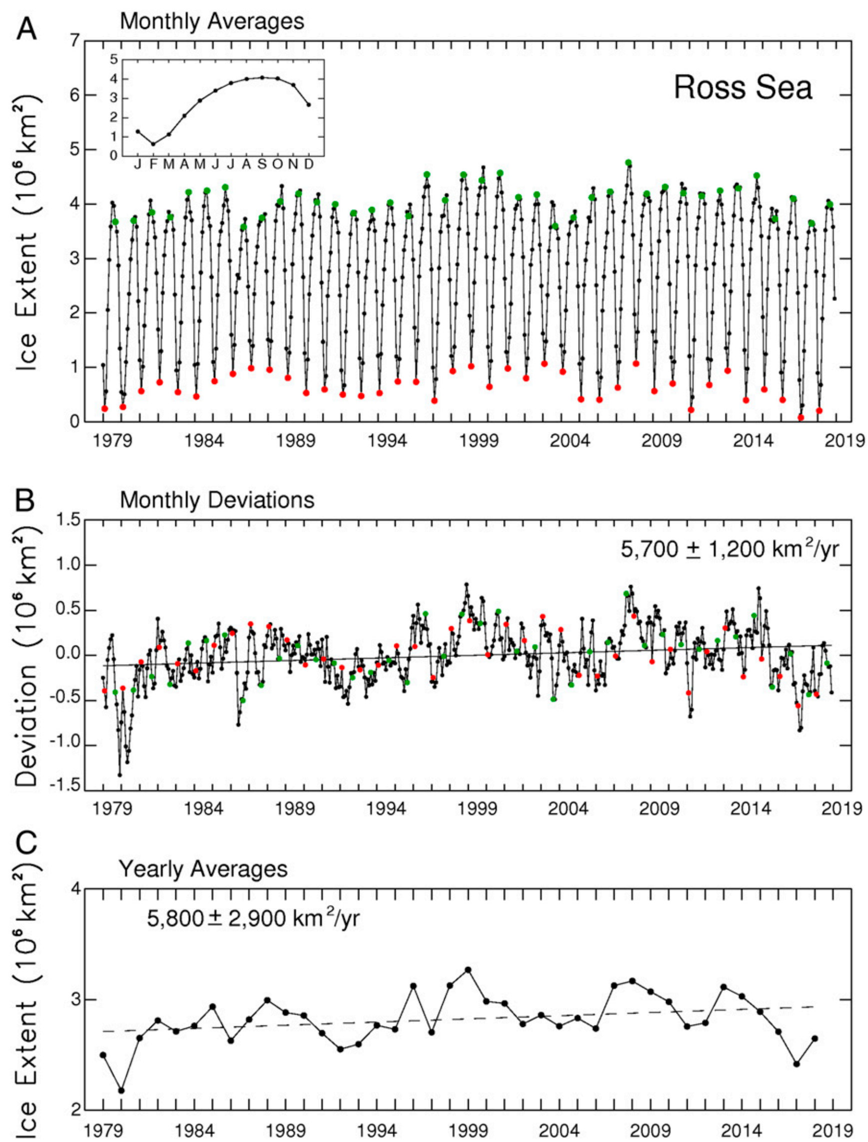

Fig. 6. (*A*) Monthly average sea ice extents in the Ross Sea, 1979–2018. February extents are colored red, September extents green, and all others black. (*Inset*) The 40-y average annual cycle. (*B*) Monthly deviations, with the line of linear least squares fit and its slope and SD. (*C*) Yearly averages and their line of linear least squares fit.

Discussion

The ice covers of each of the 5 sectors of Fig. 1 and of the Southern Ocean as a whole have experienced considerable interannual variability over the past 40 y (Figs. 2–7). In fact, the Southern Ocean and 4 of the 5 sectors (all except the Ross Sea) have each experienced at least one period since 1999 when the yearly average ice extents decreased for 3 or more straight years only to rebound again afterward and eventually reach levels exceeding the extent preceding the 3 y of decreases (Figs. 2–7). This illustrates that the ice decreases since 2014 (Fig. 2) are no assurance that the 1979–2014 overall positive trend in Southern Ocean ice extents has reversed to a long-term negative trend. Only time and an extended observational record will reveal whether the small increase in yearly average ice extents from 2017 to 2018 (Fig. 2*C*) is a blip in a long-term downward trend or the start of a rebound. Still, irrespective of what happens in the future, the 2014–2017 ice extent decreases were quite remarkable compared not only with the rest of the 40-y Antarctic record but with the Arctic record as well.

The decline in yearly average Antarctic sea ice extents from 2014 to 2017 (followed by a slight rebound) was at a linear least squares rate of $-729{,}000\ km^2 \cdot y^{-1}$, well exceeding the rate of change for either hemisphere in any other 4-y period during the 40 y (1979–2018) of the satellite multichannel passive-microwave record (Fig. 9). The widely publicized sea ice decreases in the Arctic, even with their worrisome acceleration in the early 21st century, have never experienced (in the 40-y 1979–2018 record) a 4-y period with a rate of decrease in yearly average ice extents exceeding in magnitude a value of $-240{,}000\ km^2 \cdot y^{-1}$ (Fig. 9*B*), less than a third of the Antarctic rate of loss from 2014 to 2017. In fact, the 2,027,000-km^2 decrease in yearly average Antarctic ice extents in the 3 y from their 2014 maximum (12,776,000 km^2) to their 2017 minimum (10,749,000 km^2) (Fig. 2*C*) exceeds the loss in Arctic yearly average ice extents in any period of 33 y or less in the 40-y satellite multichannel passive-microwave record. Based on the same SMMR/SSMI/SSMIS data source used for the Antarctic, the Arctic ice cover had its 40-y peak yearly average ice extent in 1982, at 12,400,000 km^2, and its minimum in 2016, at 10,135,000 km^2, for a reduction of 2,265,000 km^2 in 34 y.

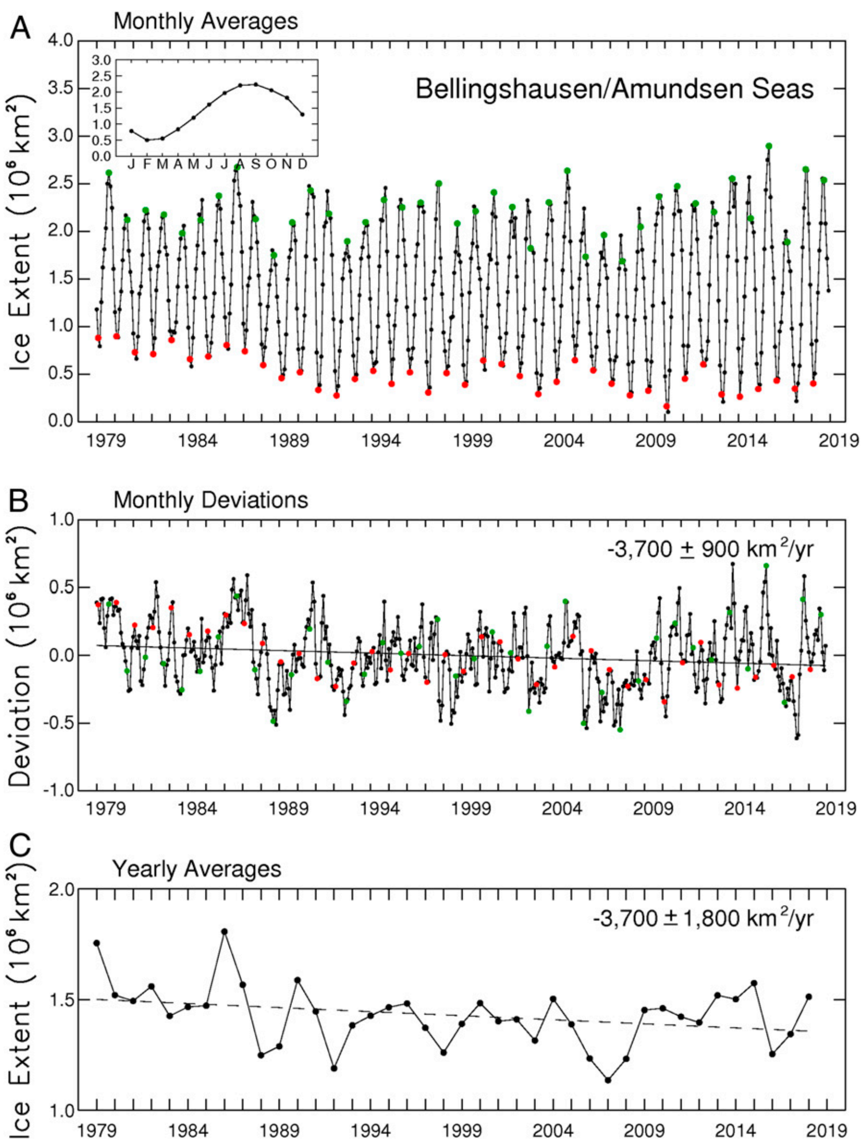

Fig. 7. (*A*) Monthly average sea ice extents in the Bellingshausen/Amundsen Seas, 1979–2018. February extents are colored red, September extents green, and all others black. (*Inset*) The 40-y average annual cycle. (*B*) Monthly deviations, with the line of linear least squares fit and its slope and SD. (*C*) Yearly averages and their line of linear least squares fit.

So, in 3 y, from 2014 to 2017, the Antarctic experienced a reduction of 89% of the total decrease of the Arctic yearly average ice extents from their maximum in 1982 to their minimum in 2016. The slope of the linear least squares fit to the 40-y Arctic yearly average ice extents is $-54{,}740 \pm 3{,}000$ $km^2 \cdot y^{-1}$, which comes to a total loss of 2,134,860 km^2 over the entire 40-y record. In just the 2014–2017 period, the Antarctic sea ice cover lost 95% of this amount.

The one other several-year period during the time frame of modern instrumental records with an estimated loss of hemispheric sea ice coverage comparably as rapid as that in the Antarctic in 2014–2017 was also in the Antarctic, although before the start of the 40-y record of multichannel passive-microwave data, coming instead in the mid-1970s. Calculations based on a variety of datasets, including satellite data, yielded 12-mo running means in Antarctic sea ice extents that show rates of decrease of ~600,000 $km^2 \cdot y^{-1}$ for the 4 y from the start of 1973 to the start of 1977 and for the 3-y subset from the start of 1974 to the start of 1977 (29). This yields an areal loss of Antarctic sea ice extents in 4 y exceeding the total loss suffered by the Arctic sea ice cover in the entire 40-y 1979–2018 satellite multichannel passive-microwave record and raises the question of whether the Antarctic sea ice might be more amenable than the Arctic sea ice to very rapid (nonannual-cycle) decreases. Certainly the geographies of the 2 polar regions are vastly different, with the Arctic sea ice cover largely confined by surrounding continents and the Antarctic sea ice wide open to water to the north, contributing to large differences also in oceanic and atmospheric circulations and offering food for thought on what might or might not be causing the differing rates of change.

Several studies have examined the extreme Antarctic sea ice retreat in late 2016 and have related it to surrounding atmospheric and oceanic conditions (30–34). Among the likely influences discussed are the following: 1) a strong northerly atmospheric flow causing rapid ice retreat in the Weddell Sea (30); 2) an unusually negative southern annular mode in November 2016 causing rapid ice retreat in the Ross Sea and elsewhere (30–34); 3) the extreme El Niño that peaked months earlier, in December 2015 through February 2016, contributing to unusually warm ocean waters in the Bellingshausen, Amundsen, and eastern Ross Seas, anomalous warmth that persisted into the

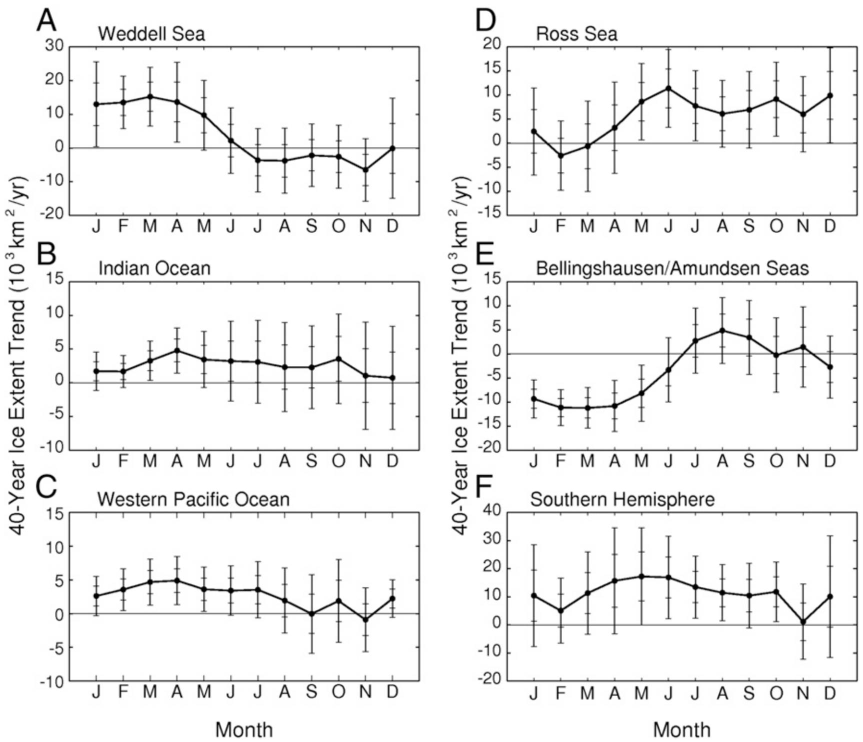

Fig. 8. Monthly sea ice extent trends over the 40-y period 1979–2018 for the following: Weddell Sea (*A*); Indian Ocean (*B*); Western Pacific Ocean (*C*); Ross Sea (*D*); Bellingshausen/Amundsen Seas (*E*); and Southern Hemisphere as a whole (*F*). The plotted trend values are the slopes of the lines of linear least squares fit, and each data point has a vertical bar with tick marks at 1 and 2 SDs above and below the trend value. Single-letter abbreviations are used for months.

austral spring (31); 4) a persistent zonal wave 3 atmospheric circulation around Antarctica contributing to reduced sea ice extents in the Indian Ocean, Ross Sea, Bellingshausen Sea, and western Weddell Sea (32–34); and 5) a weakened polar stratospheric vortex weakening the surface-level circumpolar westerlies and contributing to reduced sea ice extents in the Indian and Pacific Oceans (32). None of the studies suggests that a single cause resulted in the extreme Antarctic sea ice retreat in 2016, all instead recognizing multiple influences, both atmospheric and oceanic.

Table 2. Slopes and SDs of the lines of linear least squares fit for the Southern Ocean monthly sea ice extents, both for the 40-y record, 1979–2018, and, in parentheses, for the 36-y record, 1979–2014

Month	Slope, 10^3 $km^2 \cdot y^{-1}$	R	Slope, % per decade
January	10.4 ± 9.0 (18.4 ± 8.8)	1.15 (*2.10*)	2.2 ± 1.9 (3.9 ± 1.9)
February	5.0 ± 5.8 (13.2 ± 5.8)	0.87 (*2.25*)	1.7 ± 2.0 (4.6 ± 2.0)
March	11.3 ± 7.3 (20.6 ± 7.3)	1.54 (***2.83***)	3.0 ± 1.9 (5.6 ± 2.0)
April	15.7 ± 9.5 (24.8 ± 9.5)	1.66 (*2.60*)	2.4 ± 1.4 (3.8 ± 1.5)
May	17.3 ± 8.7 (27.9 ± 8.4)	1.99 (***3.33***)	1.8 ± 0.9 (2.9 ± 0.9)
June	16.9 ± 7.4 (26.9 ± 7.4)	*2.29* (***3.62***)	1.3 ± 0.6 (2.1 ± 0.6)
July	13.5 ± 5.5 (20.4 ± 5.7)	*2.44* (***3.55***)	0.9 ± 0.4 (1.3 ± 0.4)
August	11.4 ± 5.0 (20.1 ± 5.3)	*2.29* (***3.80***)	0.7 ± 0.3 (1.2 ± 0.3)
September	10.4 ± 5.8 (23.0 ± 5.7)	1.80 (***4.03***)	0.6 ± 0.3 (1.3 ± 0.3)
October	11.8 ± 5.3 (22.4 ± 5.2)	*2.23* (***4.30***)	0.7 ± 0.3 (1.3 ± 0.3)
November	1.1 ± 6.7 (16.2 ± 5.5)	0.17 (***2.94***)	0.1 ± 0.4 (1.0 ± 0.4)
December	10.0 ± 10.9 (34.1 ± 9.9)	0.93 (***3.46***)	1.0 ± 1.1 (3.5 ± 1.0)

The slopes and SDs are listed both as the areal loss each year and as the percentage of the ice cover lost each decade. The R column gives the ratio of the slope magnitude for the areal loss to its SD, as a rough indicator of statistical significance, both for the 40-y record and for the 36-y record. Statistical significance at the 95% level or above is indicated in the R column by italics and statistical significance at the 99% level or above is indicated by boldface.

The case studies focusing on Antarctic sea ice retreat in late 2016 illustrate well the interconnected global climate system, as they tie the sea ice changes not just to circumstances in

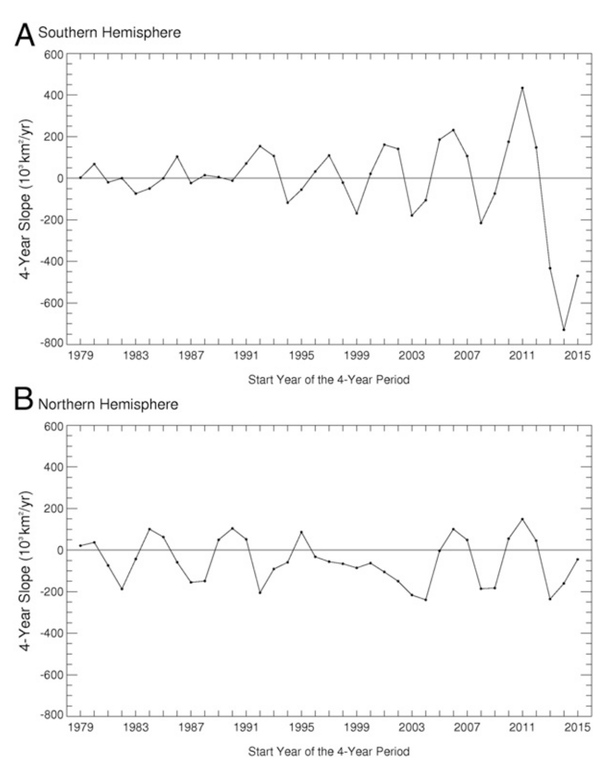

Fig. 9. Four-year slopes of the yearly average hemispheric sea ice extents, starting with the slope of the least squares fit for 1979–1982 and ending with the slope for 2015–2018, for the Southern Hemisphere (*A*) and the Northern Hemisphere (*B*).

the vicinity of the sea ice but also to events in the tropical and midlatitude oceans, the tropical and midlatitude atmosphere, and the upper atmosphere (30–34). However, the sea ice retreats in late 2016 occurred in just a few months of the 2014–2017 period of extreme rates of Antarctic sea ice decreases. I hope that the 40-y record discussed in this paper will encourage further studies into the atmospheric and oceanic conditions that could have led to the extremely rapid 2014–2017 decline of the Antarctic sea ice cover, the comparably rapid decline in the mid-1970s, and the uneven but overall gradual increases in Antarctic sea ice coverage in the intervening decades. More broadly, the environmental datasets may be nearing the point where they are long enough and rich enough to enable the linking of several of the modes and dipoles and oscillations now spoken of separately, just as the El Niño and Southern Oscillation phenomena were linked together years ago as ENSO; once that further linkage happens, the understanding of Earth's very interconnected climate system, including the sea ice cover, could be markedly enhanced.

ACKNOWLEDGMENTS. I thank Nick DiGirolamo (of Science Systems and Applications, Inc.) for his assistance in the generation of the figures. This work was funded by the NASA Earth Science Division at NASA Headquarters.

1. O. M. Johannessen, M. Miles, E. Bjorgo, The Arctic's shrinking sea ice. *Nature* **376**, 126–127 (1995).
2. C. L. Parkinson, D. J. Cavalieri, P. Gloersen, H. J. Zwally, J. C. Comiso, Arctic sea ice extents, areas, and trends, 1978-1996. *J. Geophys. Res.* **104**, 20837–20856 (1999).
3. W. N. Meier *et al*., Arctic sea ice in transformation: A review of recent observed changes and impacts on biology and human activity. *Rev. Geophys.* **51**, 185–217 (2014).
4. M. O. Jeffries, J. E. Overland, D. K. Perovich, The Arctic shifts to a new normal. *Phys. Today* **66**, 35–40 (2013).
5. J. E. Walsh, Melting ice: What is happening to Arctic sea ice, and what does it mean for us? *Oceanography* **26**, 171–181 (2013).
6. J. Stroeve, M. Holland, W. Meier, T. Scambos, M. Serreze, Arctic sea ice decline: Faster than forecast. *Geophys. Res. Lett.* **34**, L09501 (2007).
7. H. J. Zwally, J. C. Comiso, C. L. Parkinson, D. J. Cavalieri, P. Gloersen, Variability of Antarctic sea ice 1979-1998. *J. Geophys. Res.* **107**, 3041 (2002).
8. C. L. Parkinson, D. J. Cavalieri, Antarctic sea ice variability and trends, 1979-2010. *Cryosphere* **6**, 871–880 (2012).
9. I. Simmonds, Comparing and contrasting the behaviour of Arctic and Antarctic sea ice over the 35-year period 1979-2013. *Ann. Glaciol.* **56**, 18–28 (2015).
10. J. Turner, J. S. Hosking, T. J. Bracegirdle, G. J. Marshall, T. Phillips, Recent changes in Antarctic sea ice. *Philos. Trans. R. Soc. A Math. Phys. Eng. Sci.* **373**, 20140163 (2015).
11. W. R. Hobbs *et al*., A review of recent changes in Southern Ocean sea ice, their drivers and forcings. *Glob. Planet. Change* **143**, 228–250 (2016).
12. D. W. J. Thompson, S. Solomon, Interpretation of recent Southern Hemisphere climate change. *Science* **296**, 895–899 (2002).
13. J. Turner *et al*., Non-annular atmospheric circulation change induced by stratospheric ozone depletion and its role in the recent increase of Antarctic sea ice extent. *Geophys. Res. Lett.* **36**, L08502 (2009).
14. M. Sigmond, J. C. Fyfe, Has the ozone hole contributed to increased Antarctic sea ice extent? *Geophys. Res. Lett.* **37**, L18502 (2010).
15. C. M. Bitz, L. M. Polvani, Antarctic climate response to stratospheric ozone depletion in a fine resolution ocean climate model. *Geophys. Res. Lett.* **39**, L20705 (2012).
16. S. E. Stammerjohn, D. G. Martinson, R. C. Smith, X. Yuan, D. Rind, Trends in Antarctic annual sea ice retreat and advance and their relation to El Niño–Southern Oscillation and southern annular mode variability. *J. Geophys. Res.* **113**, C03S90 (2008).
17. G. A. Meehl, J. M. Arblaster, C. M. Bitz, C. T. Y. Chung, H. Tang, Antarctic sea-ice expansion between 2000 and 2014 driven by tropical Pacific decadal climate variability. *Nat. Geosci.* **9**, 590–595 (2016).
18. R. Bintanja, G. J. van Oldenborgh, S. S. Drijfhout, B. Wouters, C. A. Katsman, Important role for ocean warming and increased ice-shelf melt in Antarctic sea-ice expansion. *Nat. Geosci.* **6**, 376–379 (2013).
19. N. C. Swart, J. C. Fyfe, The influence of recent Antarctic ice sheet retreat on simulated sea ice area trends. *Geophys. Res. Lett.* **40**, 4328–4332 (2013).
20. D. J. Cavalieri, C. L. Parkinson, P. Gloersen, J. C. Comiso, H. J. Zwally, Deriving long-term time series of sea ice cover from satellite passive-microwave multisensor data sets. *J. Geophys. Res.* **104**, 15803–15814 (1999).
21. D. J. Cavalieri, C. L. Parkinson, N. DiGirolamo, A. Ivanoff, Intersensor calibration between F13 SSMI and F17 SSMIS for global sea ice data records. *IEEE Geosci. Remote Sens. Lett.* **9**, 233–236 (2012).
22. P. Gloersen *et al*., *Arctic and Antarctic Sea Ice, 1978-1987: Satellite Passive-Microwave Observations and Analysis* (National Aeronautics and Space Administration, Washington, DC, 1992).
23. J. R. Taylor, "Least-squares fitting" in *An Introduction to Error Analysis: The Study of Uncertainties in Physical Measurements* (University Science Books, Sausalito, CA, ed. 2, 1997), pp. 181–207.
24. B. D. Santer *et al*., Statistical significance of trends and trend differences in layer-average atmospheric temperature time series. *J. Geophys. Res.* **105**, 7337–7356 (2000).
25. S. N. Goodman, STATISTICS. Aligning statistical and scientific reasoning. *Science* **352**, 1180–1181 (2016).
26. D. J. Cavalieri, C. L. Parkinson, P. Gloersen, H. J. Zwally, Data from "Sea Ice Concentrations from Nimbus-7 SMMR and DMSP SSM/I-SSMIS Passive Microwave Data, Version 1." NASA National Snow and Ice Data Center Distributed Active Archive Center. https://nsidc.org/data/NSIDC-0051/versions/1. Accessed 12 February 2019.
27. D. G. Vaughan *et al*., Recent rapid regional climate warming on the Antarctic Peninsula. *Clim. Change* **60**, 243–274 (2003).
28. S. Gonzalez, D. Fortuny, How robust are the temperature trends on the Antarctic Peninsula? *Antarct. Sci.* **30**, 322–328 (2018).
29. G. Kukla, J. Gavin, Summer ice and carbon dioxide. *Science* **214**, 497–503 (1981).
30. J. Turner *et al*., Unprecedented springtime retreat of Antarctic sea ice in 2016. *Geophys. Res. Lett.* **44**, 6868–6875 (2017).
31. M. F. Stuecker, C. M. Bitz, K. C. Armour, Conditions leading to the unprecedented low Antarctic sea ice extent during the 2016 austral spring season. *Geophys. Res. Lett.* **44**, 9008–9019 (2017).
32. G. Wang *et al*., Compounding tropical and stratospheric forcing of the record low Antarctic sea-ice in 2016. *Nat. Commun.* **10**, 13 (2019).
33. E. Schlosser, F. A. Haumann, M. N. Raphael, Atmospheric influences on the anomalous 2016 Antarctic sea ice decay. *Cryosphere* **12**, 1103–1119 (2018).
34. G. A. Meehl *et al*., Sustained ocean changes contributed to sudden Antarctic sea ice retreat in late 2016. *Nat. Commun.* **10**, 14 (2019).